Supplement of Atmos. Chem. Phys., 25, 9451–9469, 2025
https://doi.org/10.5194/acp-25-9451-2025-supplement

Supplement of

Strong influence of black carbon on aerosol optical properties in central Amazonia during the fire season

Rafael Stern et al.

Correspondence to: Rafael Stern (rafa.stern@yahoo.com.br)

S1 - ACSM collection efficiency

The CE found in this study was 0.5, and it is in accordance to other studies in environments dominated by organic aerosols (Middlebrook et al., 2012; Ng et al., 2011) as well as in other studies in the Amazon (Ponczek et al., 2021; de Sá et al., 2019). However, it was different from the CE during the wet season in the same site as in our study (CE=1, (Chen et al., 2015), and from an area highly impacted by local fires (CE = 1, (Brito et al., 2014)). To convert the integrated volume of the SMPS measurements to mass concentration the density of the compounds was considered 1.78 g cm^{-3} for SO_4, 1.77 g cm^{-3} for eBC, 1.72 g cm^{-3} for NH_4 and NO_3, and 1.48 g cm^{-3} for the organics (Brito et al., 2014). The mean density of all the PM1 aerosols measured in our study was 1.54±0.02 g cm^{-3} and was multiplied by the total volume estimated from the SMPS measurements to obtain the integral mass.

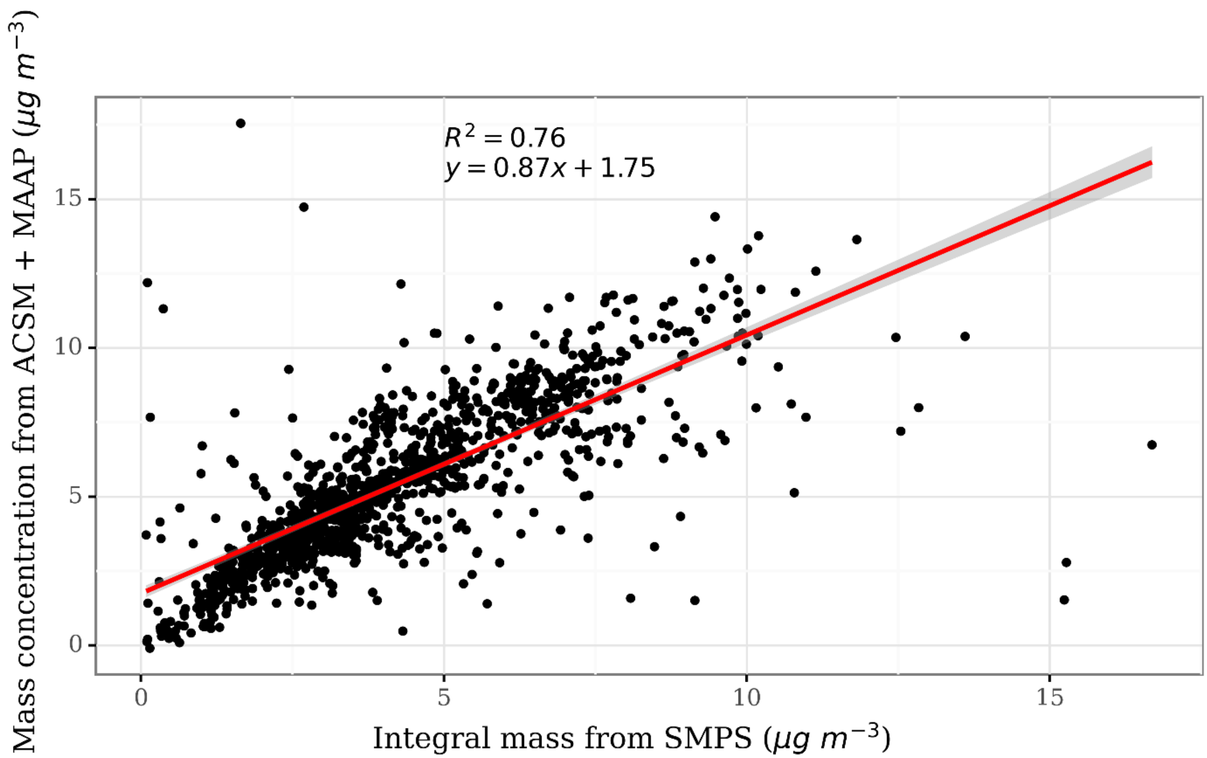

Figure S1 – Collection efficiency validation combining the mass concentration of non-refractary submicrometer particles (ACSM) and eBC (MAAP) with the integral mass from the SMPS.

S2 – Generator filter by wind direction

Time series of the fBC, where gray points represent data which passed the filter criteria and was included in the results, and black points represent the data which was filtered out of the analysis because if was the criteria of either the wind direction was between 270-340° (for local diesel generator contamination, from our local wind direction measurements) or when the calculated backtrajectories from the Hysplit model (Draxler and Hess, 1998) passed over Manaus coordinates, as in (Whitehead et al., 2016). About 17% of the data was filteres out in this process.

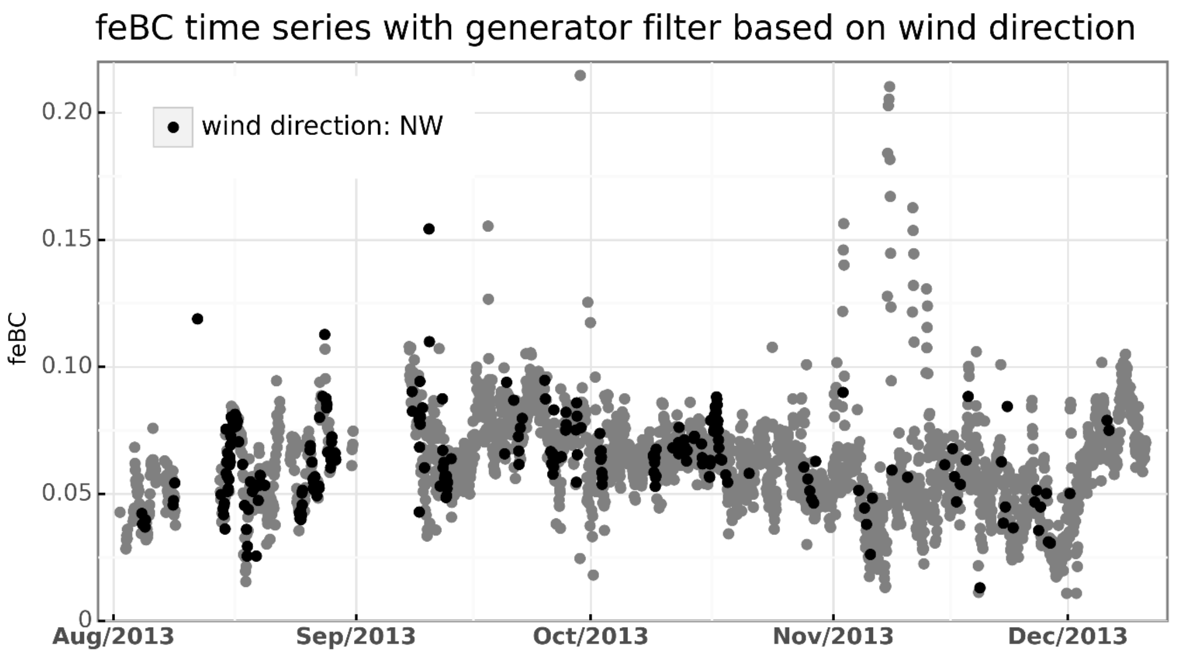

Figure S2 – Time series of the fBC, where black dots indicate the data points filtered out due possible contamination from pollution from Manaus or/and the generator.

S3 - PMF factors

S3.1 - Signal fractions

Table S1 – Comparison of different parameters of validation of the nmber of PMF factors

Number of factors	Q/Q expected	fPeak or seed
3	0.31	-0.2
4	0.29	0

S3.1.1 - 3 Factors solution

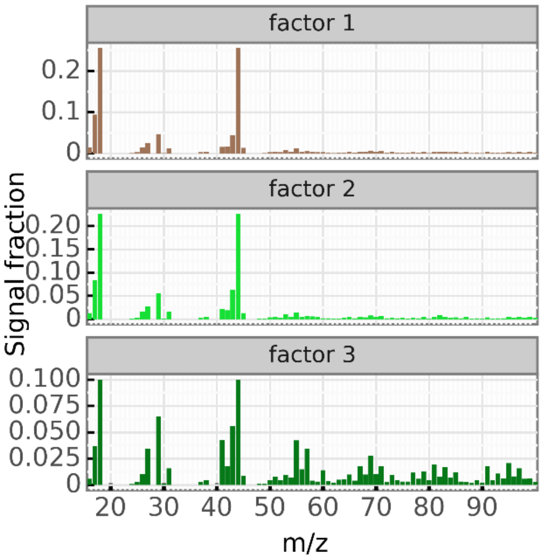

Figure S3 – Signal fractions of the PMF for a 3 factors solution.

S3.1.2 - 4 factors solution

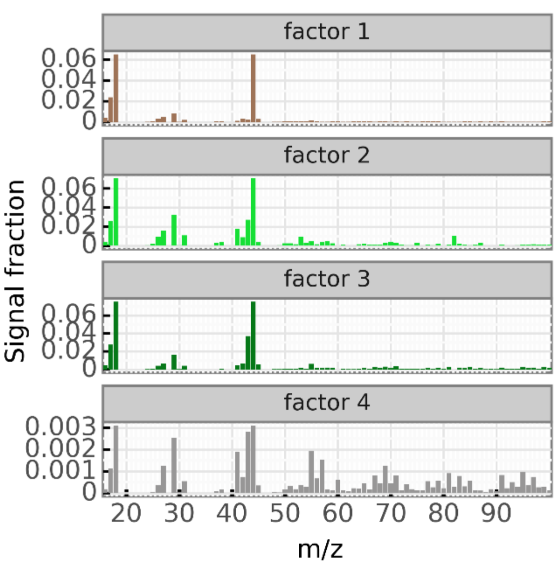

Figure S4 – Signal fractions of the PMF for a 4 factors solution.

S3.2 - Pearson`s R

S3.2.1 - 3 factors

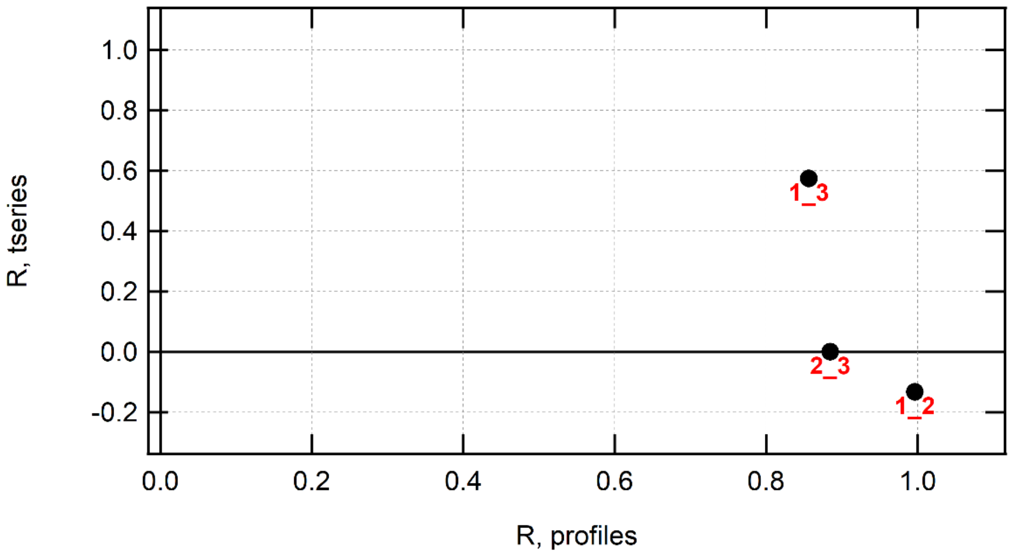

Figure S5 – Pearson`s R for the correlations between the time series and the mass spectra of any 2 factors for the PMF solutions with 3 factors.

S3.2.2 - 4 factors

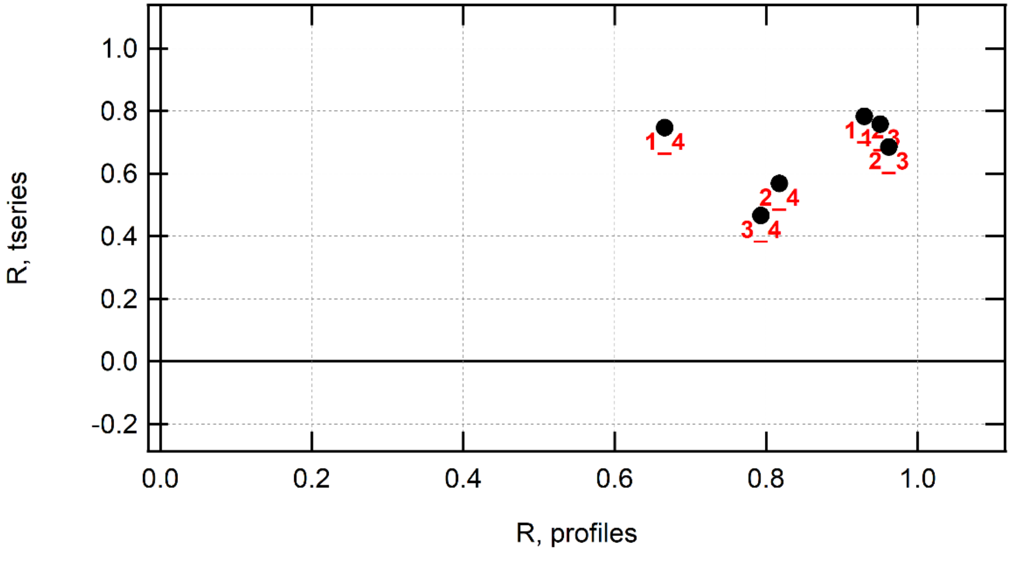

Figure S6 – Pearson`s R for the correlations between the time series and the mass spectra of any 2 factors for the PMF solutions with 4 factors.

S3.3 - Scaled residuals for all m/z`s

S3.3.1 - 3 factors solution

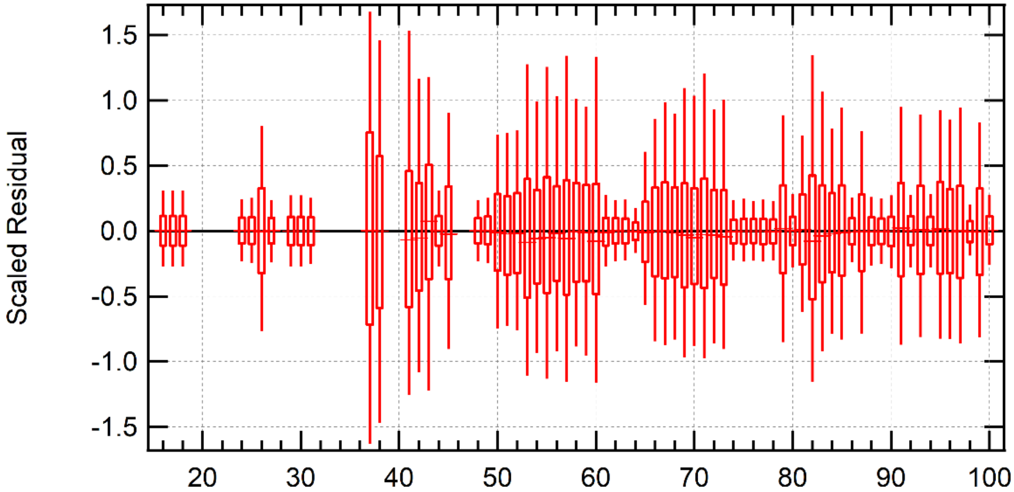

Figure S7 – Scaled residuals for the PMF solution with 3 factors.

S3.3.2 - 4 factors solution

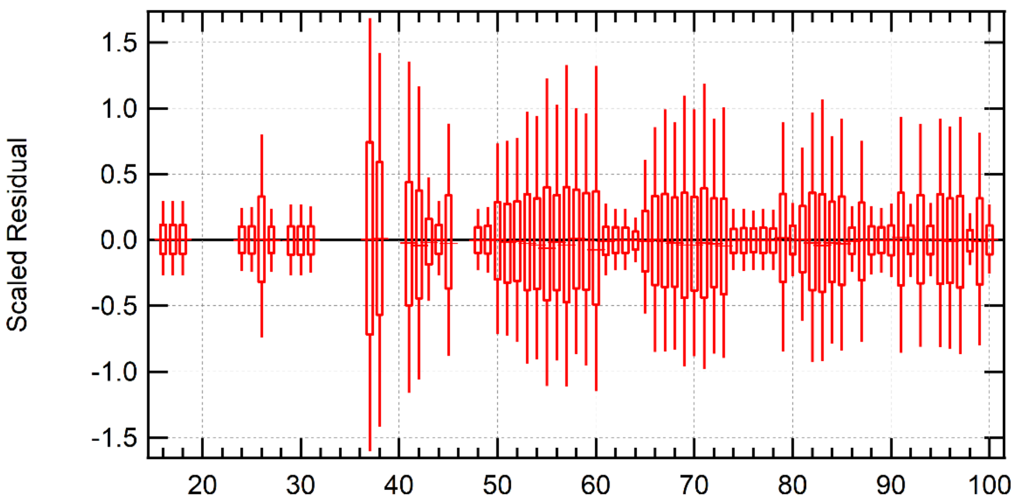

Figure S8 – Scaled residuals for the PMF solution with 4 factors.

S3.4 - Diel cycles

S3.4.1 - 3 factors

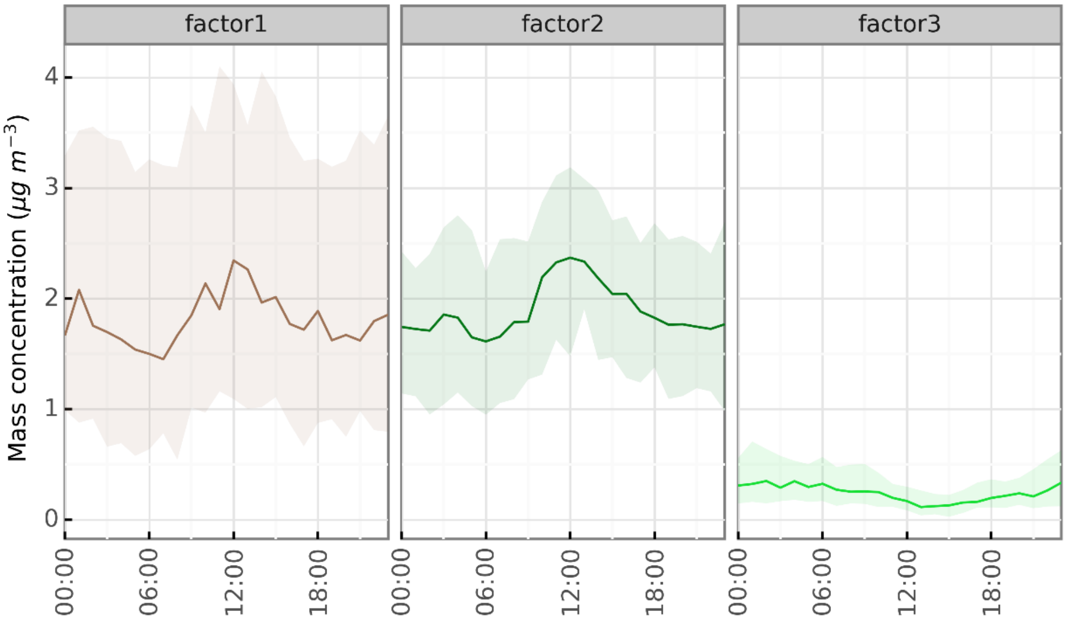

Figure S9 – Diel cycles of the different PMF factors for a 3 factors solution.

S3.4.2 - 4 factors

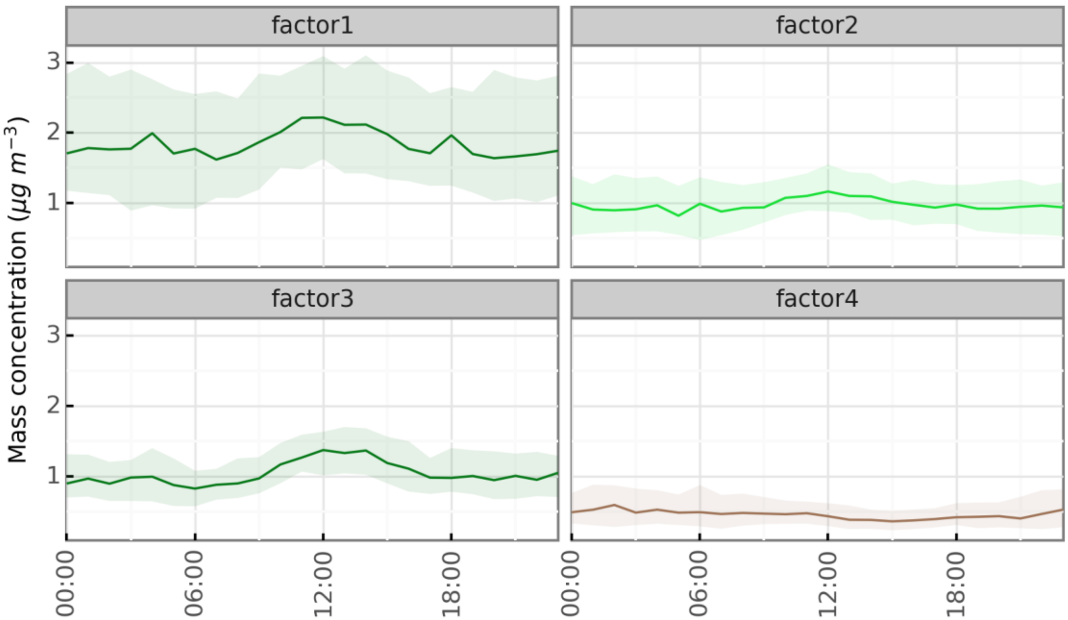

Figure S10 – Diel cycles of the different PMF factors for a 4 factors solution.

S4 - Correlation matrixes

S4.1 - 3 factor solution based on 4 factors solution, with 2 combined:

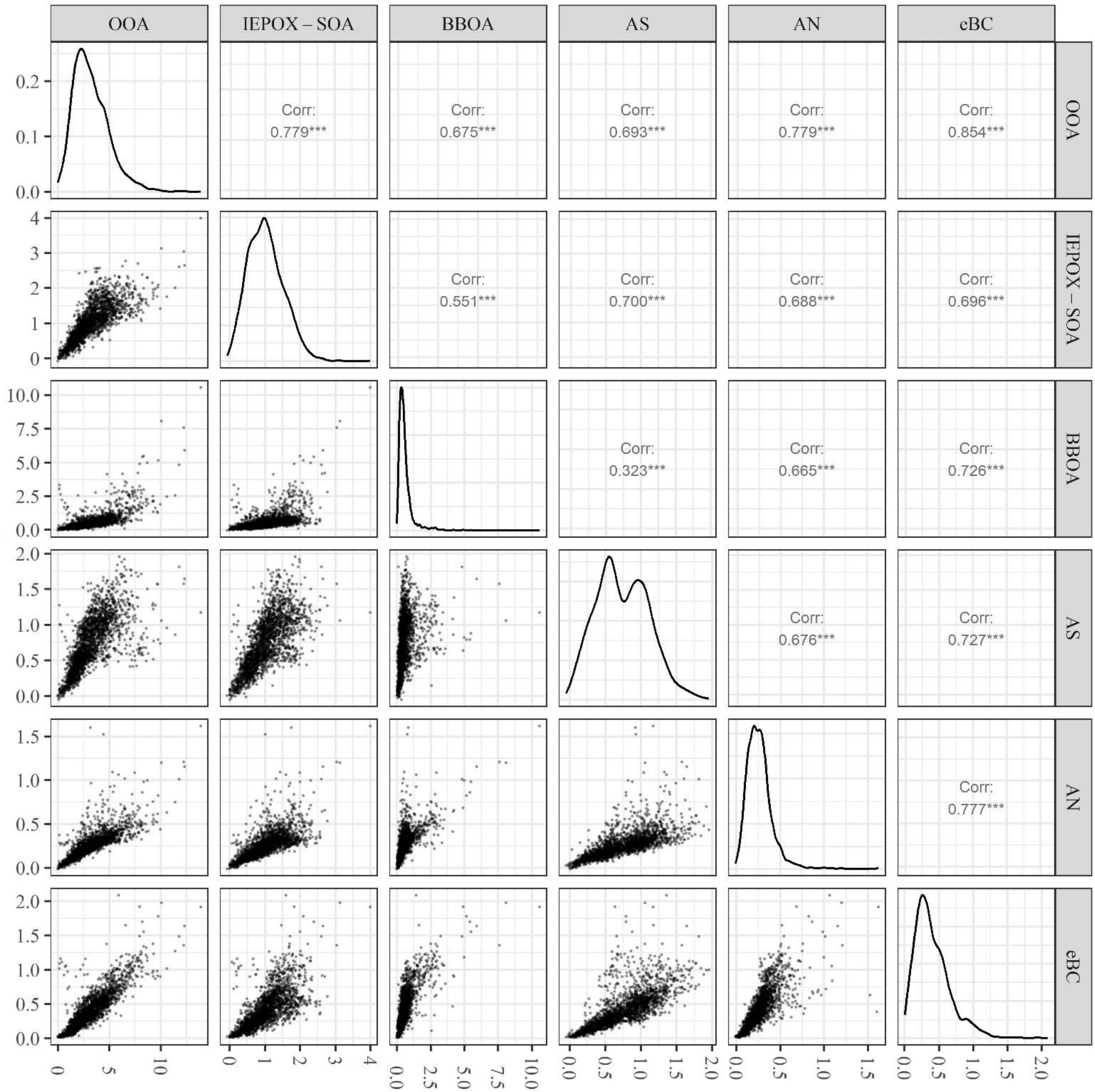

Figure S11 - Correlation matrix of all the aerosol species for a 3 factor solution based on 4 factors solution, with 2 combined. The numbers are the Pearson values, and the ‘***’ means that $p < 0.001$.

S4.2 - 3 factor solution:

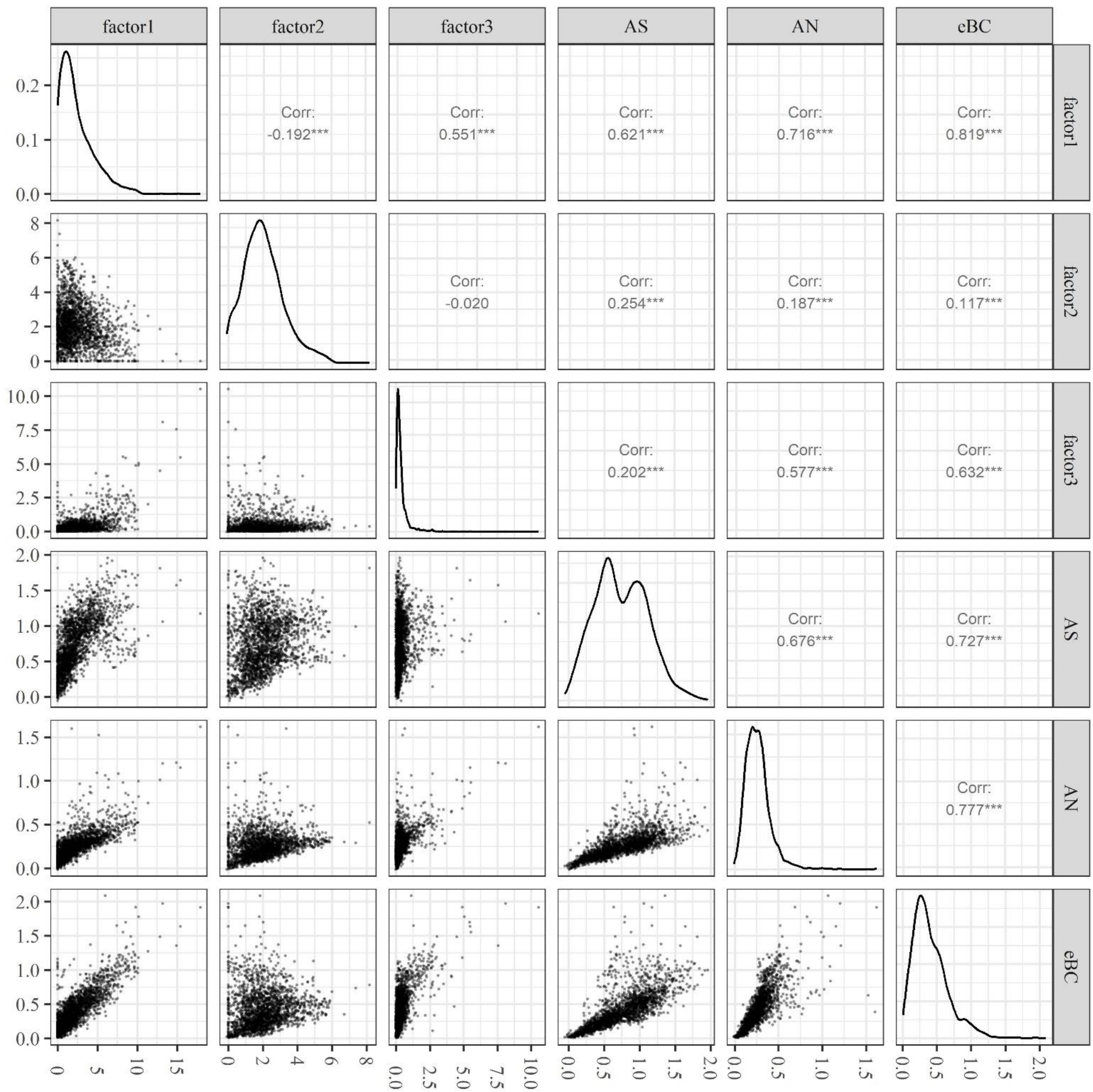

Figure S12 - Correlation matrix of all the aerosol species for a 3 factors solution. The numbers are the Pearson values, and the '***' means that $p < 0.001$.

S4.3 - 4 factor solution, factors 1 and 3 were combined to generate the combined 3 factors solution:

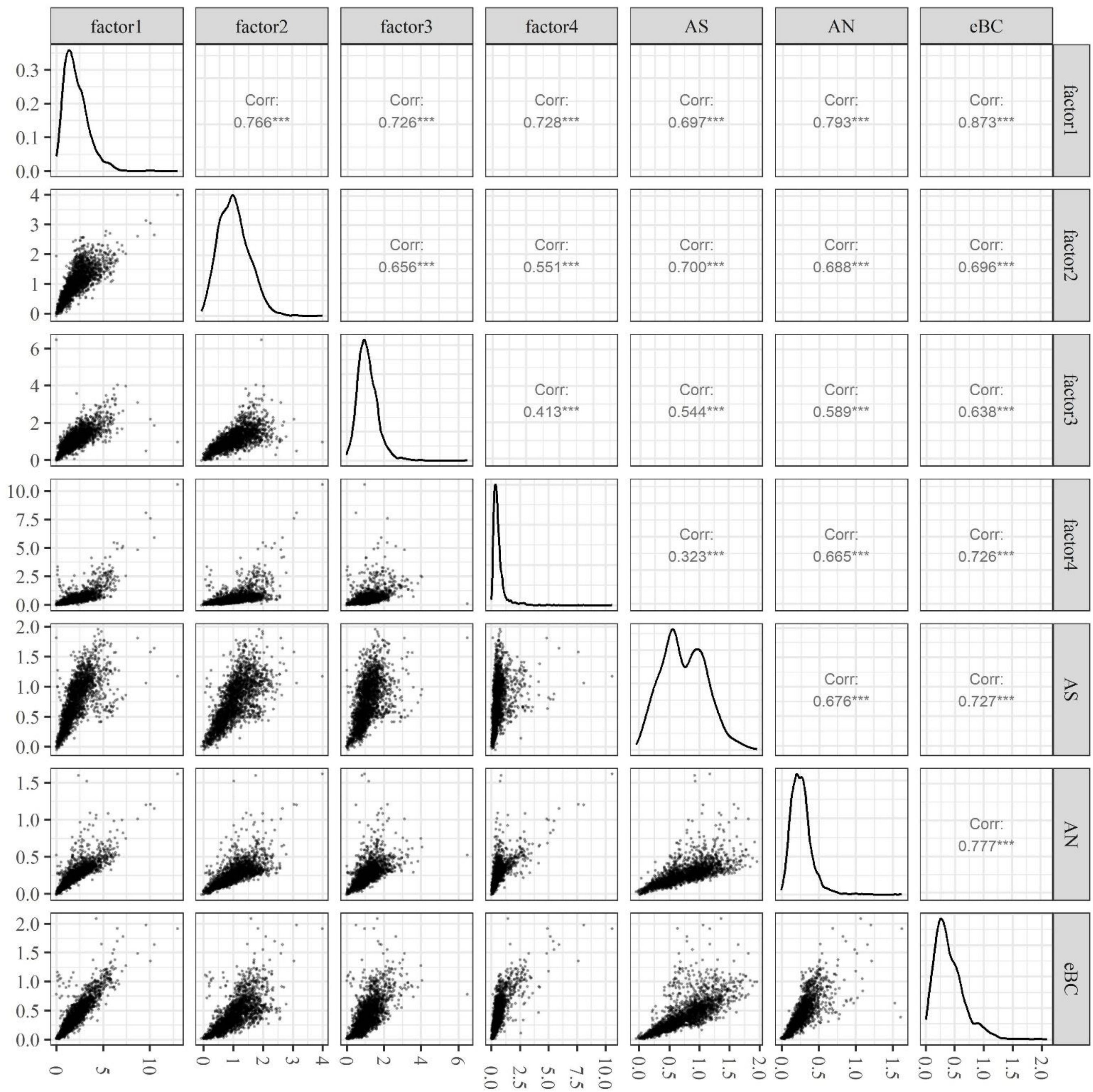

Figure S13 - Correlation matrix of all the aerosol species for a 4 factors solution. The numbers are the Pearson values, and the '***' means that $p < 0.001$.

S5 - Multi-linear regression model tests

Table S2 - Testing the MLR without AN.

	MSE ($m^2\ g^{-1}$)							
Wavelength (nm)	450	450 test	550	550 test	637	637 test	700	700 test
eBC	13.58±1.08	13.81±1.08	10.67±0.70	10.84±0.71	8.68±0.52	8.82±0.53	7.62±0.44	7.78±0.45
BBOA	7.96±0.33	8.49±0.31	5.33±0.21	5.72±0.20	3.83±0.16	4.16±0.15	3.10±0.13	3.40±0.13
IEPOX-SOA	5.61±0.41	5.76±0.41	3.84±0.27	3.95±0.27	2.87±0.20	2.97±0.20	2.37±0.17	2.43±0.17
OOA	3.58±0.15	3.74±0.15	1.94±0.10	2.05±0.10	1.24±0.07	1.34±0.07	0.90±0.06	0.99±0.06
AS	4.79±0.62	5.80±0.60	4.79±0.41	5.53±0.39	4.77±0.30	5.41±0.29	4.58±0.25	5.11±0.25
R^2	0.92	0.92	0.93	0.93	0.93	0.93	0.93	0.92

Table S3 - Mean of 100 tests using different randomly selected subsets of 50% of the data.

	MSE ($m^2\ g^{-1}$)							
Wavelength (nm)	450	450 test	550	550 test	637	637 test	700	700 test
eBC	13.58±1.08	13.86±2.77	10.67±0.70	10.85±1.77	8.68±0.52	8.81±1.28	7.62±0.44	7.75±1.07
BBOA	7.96±0.33	7.90±1.07	5.33±0.21	5.28±0.74	3.83±0.16	3.79±0.56	3.10±0.13	3.07±0.47
IEPOX-SOA	5.61±0.41	5.49±0.56	3.84±0.27	3.76±0.37	2.87±0.20	2.81±0.27	2.37±0.17	2.30±0.23
OOA	3.58±0.15	3.56±0.31	1.94±0.10	1.92±0.22	1.24±0.07	1.23±0.16	0.90±0.06	0.89±0.14
AS	4.79±0.62	4.89±1.40	4.79±0.41	4.87±0.89	4.77±0.30	4.83±0.64	4.58±0.25	4.62±0.52

AN	7.07±1.41	7.14±2.20	5.17±0.92	5.26±1.51	4.41±0.68	4.50±1.20	3.93±0.58	4.01±1.05
R^2	0.92	0.92±0.01	0.93	0.93±0.01	0.93	0.93±0.01	0.93	0.93±0.01

S6 – MSE for eBC MAC = 12.3 m^2 g^{-1}

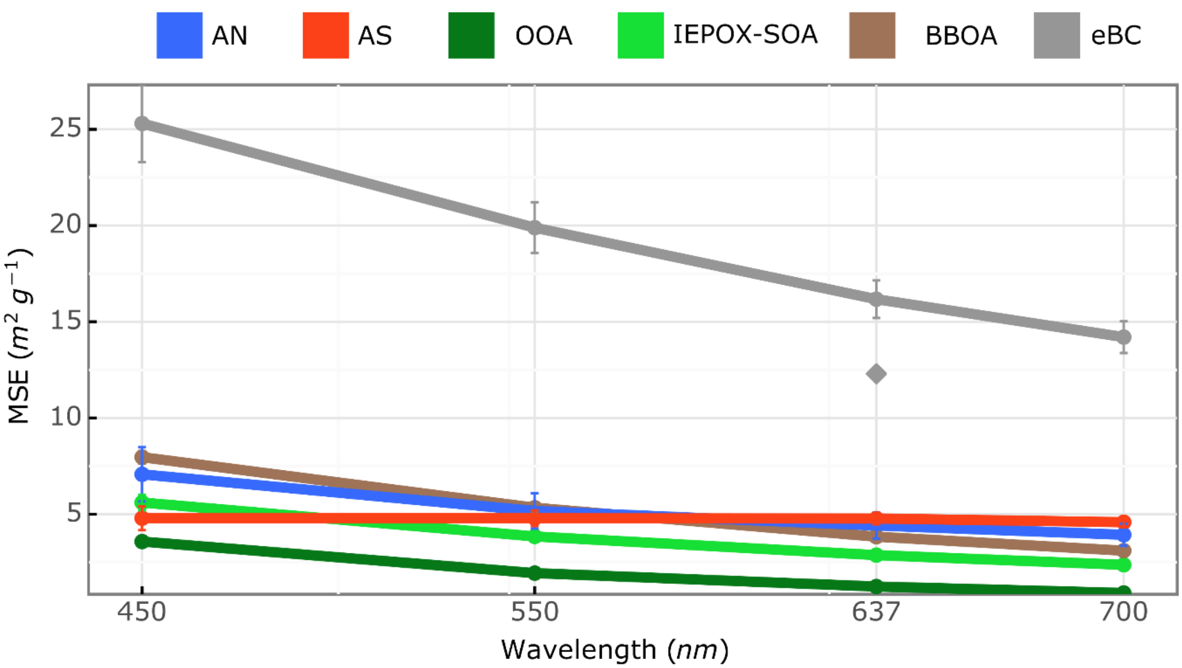

Figure S14 - Mass scattering efficiencies (MSE) for each chemical component at each wavelength, based on mass absorption cross-section values for eBC = 12.3 m^2 g^{-1} (Saturno et al., 2018).

Table S4 – MSE (m^2 g^{-1}), MEE (m^2 g^{-1}), SSA and mass concentration (μg m^{-3}) of eBC particles based on mass absorption cross-section values for eBC = 12.3 m^2 g^{-1} (Saturno et al., 2018). The R^2 of the MSE was 0.92-0.93, and all $p < .001$.

	MSE (m^2 g^{-1})				SSA	Mass concentration (μg m^{-3})
Wavelength (nm)	450	550	637	700		
eBC	25.30±2.00	19.88±1.31	16.17±0.97	14.20±0.83	0.57	0.22±0.14

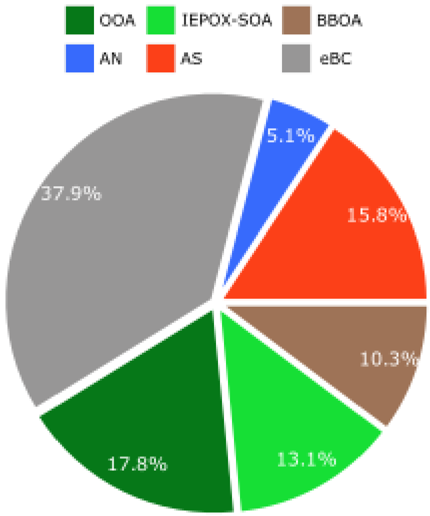

Figure S15 - The relative contribution (%) of extinction coefficient (scattering + absorption) of each component considering its mass fraction to the total mass of submicrometer particles, based on mass absorption cross-section values for eBC = 12.3 $m^2\ g^{-1}$ (Saturno et al., 2018).

References

Brito, J., Rizzo, L. V., Morgan, W. T., Coe, H., Johnson, B., Haywood, J., Longo, K., Freitas, S., Andreae, M. O. and Artaxo, P.: Ground-based aerosol characterization during the South American Biomass Burning Analysis (SAMBBA) field experiment, Atmos. Chem. Phys., 14(22), 12069–12083, doi:10.5194/acp-14-12069-2014, 2014.

Chen, Q., Farmer, D. K., Rizzo, L. V., Pauliquevis, T., Kuwata, M., Karl, T. G., Guenther, a., Allan, J. D., Coe, H., Andreae, M. O., Pöschl, U., Jimenez, J. L., Artaxo, P. and Martin, S. T.: Submicron particle mass concentrations and sources in the Amazonian wet season (AMAZE-08), Atmos. Chem. Phys., 15(7), 3687–3701, doi:10.5194/acp-15-3687-2015, 2015.

Draxler, R. R. and Hess, G. D.: An overview of the HYSPLIT_4 modelling system for trajectories, dispersion and deposition, Aust. Meteorol. Mag., 47(4), 295–308, 1998.

Middlebrook, A. M., Bahreini, R., Jimenez, J. L. and Canagaratna, M. R.: Evaluation of Composition-Dependent Collection Efficiencies for the Aerodyne Aerosol Mass Spectrometer using Field Data, Aerosol Sci. Technol., 46(3), 258–271, doi:10.1080/02786826.2011.620041, 2012.

Ng, N. L., Herndon, S. C., Trimborn, A., Canagaratna, M. R., Croteau, P. L., Onasch, T. B., Sueper, D., Worsnop, D. R., Zhang, Q., Sun, Y. L. and Jayne, J. T.: An Aerosol Chemical Speciation Monitor (ACSM) for routine monitoring of the composition and mass concentrations of ambient aerosol, Aerosol Sci. Technol., 45(7), 780–794, doi:10.1080/02786826.2011.560211, 2011.

Ponczek, M., Franco, M. A., Carbone, S., Rizzo, L. V., Monteiro dos Santos, D., Morais, F. G., Duarte, A., Barbosa, H. M. J. and Artaxo, P.: Linking the chemical composition and optical properties of biomass burning aerosols in Amazonia, Environ. Sci. Atmos., 2(2), 252–269, doi:10.1039/d1ea00055a, 2021.

de Sá, S. S., Rizzo, L. V., Palm, B. B., Campuzano-Jost, P., Day, D. A., Yee, L. D., Wernis, R., Isaacman-VanWertz, G., Brito, J., Carbone, S., Liu, Y. J., Sedlacek, A., Springston, S., Goldstein, A. H., Barbosa, H. M. J., Alexander, M. L., Artaxo, P., Jimenez, J. L. and Martin, S. T.: Contributions of biomass-burning, urban, and biogenic emissions to the concentrations and light-absorbing properties of particulate matter in central Amazonia during the dry season, Atmos. Chem. Phys., 19(12), 7973–8001, doi:10.5194/acp-19-7973-2019, 2019.

Saturno, J., Holanda, B. A., Pöhlker, C., Ditas, F., Wang, Q., Moran-Zuloaga, D., Brito, J., Carbone, S., Cheng, Y., Chi, X., Ditas, J., Hoffmann, T., Hrabe De Angelis, I., Könemann, T., Lavrič, J. V., Ma, N., Ming, J., Paulsen, H., Pöhlker, M. L., Rizzo, L. V., Schlag, P., Su, H., Walter, D., Wolff, S., Zhang, Y., Artaxo, P., Pöschl, U. and Andreae, M. O.: Black and brown carbon over central Amazonia: Long-term aerosol measurements at the ATTO site, Atmos. Chem. Phys., 18(17), 12817–12843, doi:10.5194/acp-18-12817-2018, 2018.

Whitehead, J. D., Darbyshire, E., Brito, J., Barbosa, H. M. J., Crawford, I., Stern, R., Gallagher, M. W., Kaye, P. H., Allan, J. D., Coe, H., Artaxo, P. and McFiggans, G.: Biogenic cloud nuclei in the central Amazon during the transition from wet to dry season, Atmos. Chem. Phys., 16(15), 9727–9743, doi:10.5194/acp-16-9727-2016, 2016.